ARTICLE

OBC
www.rsc.org/obc

Synthesis, stability and bonding situation of tris-, bis- and mono[9-(azuleno[1,2-*b*]thienyl)]methyl cations †

Shunji Ito,*[a] Takahiro Kubo,[a] Mao Kondo,[a] Chizuko Kabuto,[a] Noboru Morita,[a] Toyonobu Asao,[a] Kunihide Fujimori,[b] Masataka Watanabe,[c] Nobuyuki Harada[c] and Masafumi Yasunami[d]

[a] *Department of Chemistry, Graduate School of Science, Tohoku University, Sendai 980-8578, Japan. E-mail: ito@funorg.chem.tohoku.ac.jp*

[b] *Department of Chemistry, Faculty of Science, Shinshu University, Matsumoto 390-8621, Japan*

[c] *Institute of Multidisciplinary Research for Advanced Materials, Tohoku University, Sendai 980-8577, Japan*

[d] *Department of Materials Science and Engineering, College of Engineering, Nihon University, Koriyama 963-1165, Japan*

Received 10th March 2003, Accepted 28th May 2003
First published as an Advance Article on the web 10th June 2003

Stable tris-, bis- and mono[9-(azuleno[1,2-*b*]thienyl)]methyl cations (**7a**, **8a** and **9a**) and their derivatives, with a 6-isopropyl substituent on each azuleno[1,2-*b*]thiophene ring (**7b**, **8b** and **9b**) were prepared by the hydride abstraction reaction of the corresponding methane derivatives. The bonding situation of these compounds including the methane derivatives was examined by analysis of the ^3J(H,H) values for the seven-membered ring from the ^{1}H NMR spectra. The methane derivatives exhibited a significant alternating pattern in the ^3J(H,H) values, which indicated that the π-system of the azulene core is perturbed by the fused thiophene ring, showing a tendency towards a localized heptafulvene substructure. The ^3J(H,H) values of **7b** and **8b** in the seven-membered ring revealed that the alternating C–C bond lengths in the azulene core still existed. The cations **9a** and **9b**, which exhibited nearly equal ^3J(H,H) values in the seven-membered ring, exhibit the development of a delocalized tropylium substructure in the azulene core. X-ray crystal analysis of 6-isopropylazuleno[1,2-*b*]thiophene revealed substantial bond-length alternation in the seven-membered ring. Significant bond-length equalization in the seven-membered ring was also confirmed by the X-ray crystal analysis of **9b**. The stability of these carbocations was examined by measurement of the pK_R^+ values and the redox potentials, which revealed that the bond-length alternation in the azulene core does not significantly affect the stability of the carbocations.

Introduction

Azulene ($C_{10}H_8$)[1] shows nearly equal bond lengths (1.387–1.404 Å) around its 10π-electron periphery owing to peripheral delocalization.[2] However, condensation of an aromatic ring with azulene at its five-membered ring, *e.g.*, benz[*a*]azulene (**1a**) or azuleno[1,2-*b*]thiophene (**2a**),[3] exhibits remarkable alternating carbon–carbon bond lengths in the seven-membered ring, which are revealed by ^{1}H NMR analysis[4,5] and X-ray structure analysis[6,7] of such compounds. Moreover, recently, the azulene (**3**) fused with oxabicyclo[2.2.1]heptadiene at the seven-membered ring exhibits marked bond-length alternation in the azulene system (Chart 1).[8]

There are numerous reports concerning stabilized (1-azulenyl)methyl cations in the literature.[1a] We have also reported the synthesis of a series of (1-azulenyl)methylium hexafluorophosphates, *i.e.*, tri(1-azulenyl)methylium, di(1-azulenyl)phenylmethylium and (1-azulenyl)diphenylmethylium hexafluorophosphates (**4a**·PF_6^-, **5a**·PF_6^- and **6a**·PF_6^-) and their derivatives (*e.g.*, **4b**,**c**·PF_6^-, **5b**,**c**·PF_6^- and **6b**,**c**,·PF_6^-) by the hydride abstraction of the corresponding hydrocarbons (Chart 2).[9] However, to the best of our knowledge, little is known about the carbocations constructed by the condensed-ring compounds of azulene.

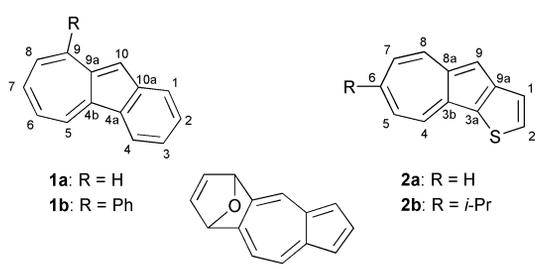

Chart 1

The bond-length alternation should be affected by the charge distribution on the azulene ring. It is known that the introduction of an electron-withdrawing group into the five-membered ring of the condensed-ring compounds of azulene reduces the bond-length alternation owing to the contribution of the dipole resonance structure.[10] However, it has not been clarified how the bond-length alternation is reduced. Herein we report the first synthesis of a series of (1-azulenyl)methyl cations (**7a**, **8a** and **9a**) produced by azuleno[1,2-*b*]thiophene (**2a**) in order to investigate the bonding situation in the series of carbocation systems (Chart 3). Since the ^{1}H NMR coupling constants have been proven useful in understanding the bonding situation of similar molecules,[6,8] we have also synthesized 6-isopropyl derivatives (**7b**, **8b** and **9b**) for the unequivocal analysis of the NMR spectra in the seven-membered ring, the results of which are also reported herein. The bonding situation was also revealed by the X-ray crystal analyses of 6-isopropylazuleno[1,2-*b*]-

† Electronic supplementary information (ESI) available: CV waves of compounds **7a**, **8a** and **9a**, redox details of compounds **7a**,**b**, **8a**,**b**, and **9a**,**b** along with those of **4a**, **5a** and **6a**, ORTEP drawings and details of the X-ray analyses of compounds **2b** and **9b** and NMR details of the compounds reported. See http://www.rsc.org/suppdata/ob/b3/b302688d/

DOI: 10.1039/b302688d

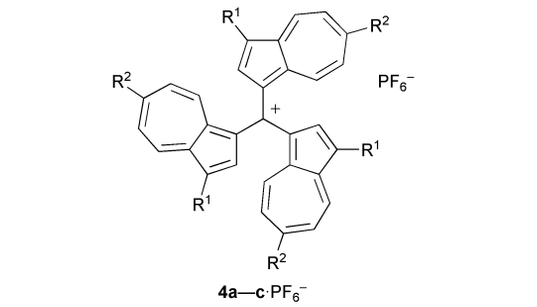

4a—c·PF_6^-

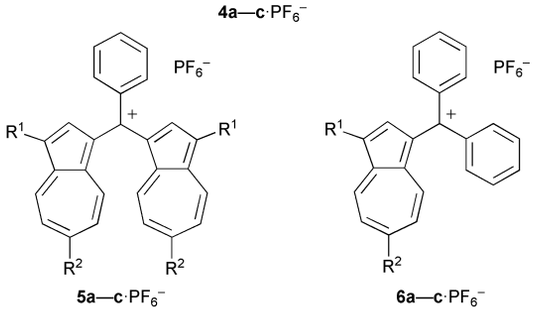

5a—c·PF_6^- **6a—c**·PF_6^-

a: $R^1 = R^2 = H$, **b**: $R^1 = Me$, $R^2 = H$, **c**: $R^1 = R^2 = t$-Bu

Chart 2

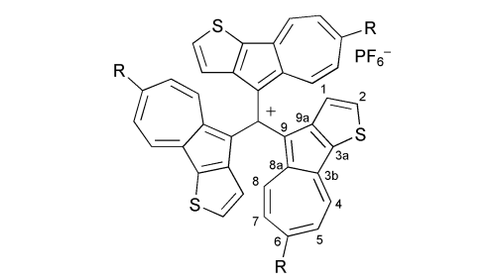

7a,b·PF_6^-

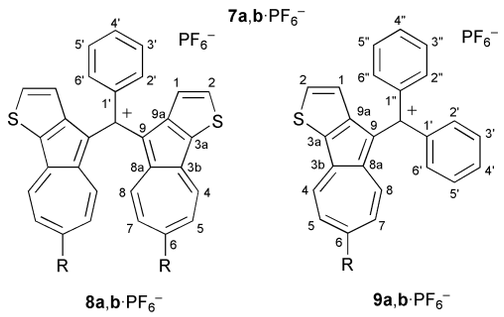

8a,b·PF_6^- **9a,b**·PF_6^-

a: R = H, **b**: R = *i*-Pr

Chart 3

thiophene (**2b**) and the cation **9b**. The stability of the carbocations was examined by measurement of the pK_{R^+} values and the redox potentials upon cyclic voltammetry (CV).

Results and discussion

The isopropyl derivative of azuleno[1,2-*b*]thiophene (**2b**) was prepared using a similar procedure to the synthesis of **2a**, starting from 6-isopropyl-2*H*-cyclohepta[*b*]furan-2-one (**10**)[11] as illustrated in Scheme 1. The reaction of two molar amounts of **2a**,**b** with 9-azuleno[1,2-*b*]thiophenecarbaldehydes (**15a**,**b**) (which were prepared by Vilsmeier reaction of **2a**,**b** in 93% and 86% yields, respectively) in acetic acid at room temperature afforded **16a**,**b** in 76% and 42% yields, respectively. Hydride abstraction reaction of **16a**,**b** with DDQ in dichloromethane at room temperature proceeded under the conditions similar to those employed for the formation of **4a**–**c**.[9d] Addition of a 60% HPF_6 solution to the reaction mixture yielded the desired tris(9-azuleno[1,2-*b*]thienyl)methyl cations (**7a**,**b**) as hexafluorophosphates in 86% and 75% yields, respectively (Scheme 2).

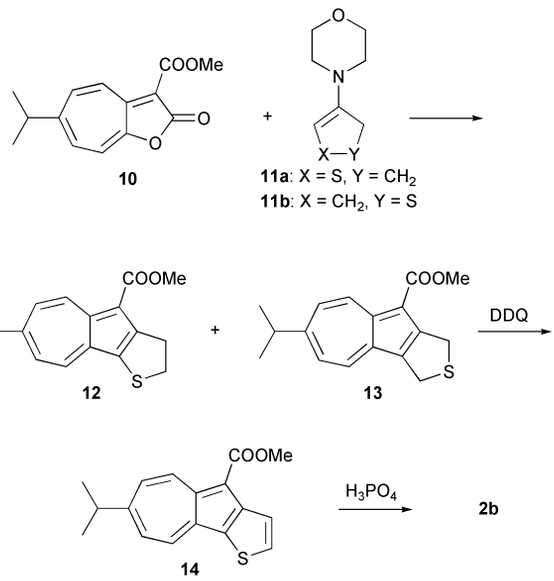

10 **11a**: X = S, Y = CH_2 **11b**: X = CH_2, Y = S

12 **13** **14** **2b**

Scheme 1

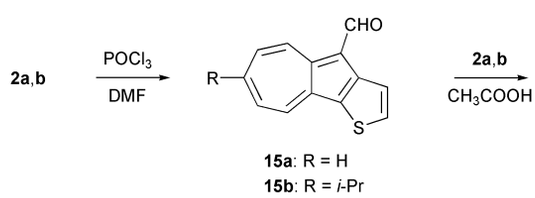

15a: R = H **15b**: R = *i*-Pr

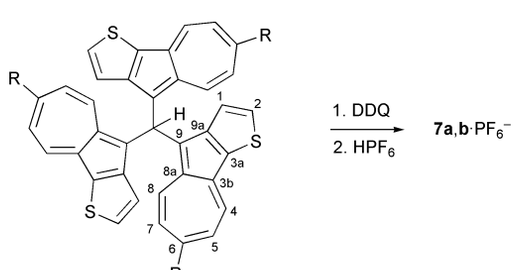

16a: R = H **16b**: R = *i*-Pr

Scheme 2

The reaction of two molar amounts of **2a**,**b** with benzaldehyde (**17**) in acetic acid at room temperature afforded **18a**,**b** in 91% and 82% yields, respectively. Hydride abstraction reaction of **18a**,**b** with DDQ in dichloromethane at room temperature, followed by the addition of an HPF_6 solution, afforded bis(9-azuleno[1,2-*b*]thienyl)phenylmethylium hexafluorophosphates **8a**,**b**·PF_6^- in 81% and 63% yields, respectively (Scheme 3).

The reaction of **2a**,**b** with benzhydrol (**19**) in warming acetic acid afforded **20a**,**b** in 44% and 41% yields, respectively. Hydride abstraction reaction of **20a**,**b** with DDQ, followed by the addition of an HPF_6 solution, yielded (9-azuleno[1,2-*b*]thienyl)diphenylmethylium hexafluorophosphates **9a**,**b**·PF_6^- in 82% and 95% yields, respectively (Scheme 4).

Mass spectra of **7a**,**b**·PF_6^-, **8a**,**b**·PF_6^- and **9a**,**b**·PF_6^- ionized by FAB showed the correct $M^+ - PF_6$ ion peak. The characteristic bands of hexafluorophosphate were observed at 837–839 (strong) and 558 (medium) cm^{-1} in the IR spectra. These salts showed strong absorption in the visible region in analogy with the salts **4a**·PF_6^-, **5a**·PF_6^- and **6a**·PF_6^- and their congeners.[9] The longest wavelength absorption maxima (nm) and their coefficients (log ε) of the hexafluorophosphates in the visible region are summarized in Table 1. UV–vis spectra of **7a**·PF_6^-, **8a**·PF_6^- and **9a**·PF_6^- in acetonitrile are shown in Fig. 1. As

Table 1 The longest wavelength absorptions and coefficients of **7a**,**b**·PF_6^-, **8a**,**b**·PF_6^- and **9a**,**b**·PF_6^- in acetonitrile

Sample	λ_{max}, nm (log ε)	Sample	λ_{max}, nm (log ε)
7a·PF_6^-	691 (4.67)	**7b**·PF_6^-	709 (4.66)
8a·PF_6^-	718 (4.54)	**8b**·PF_6^-	721 (4.46)
9a·PF_6^-	486 (4.26)	**9b**·PF_6^-	481 (4.17)

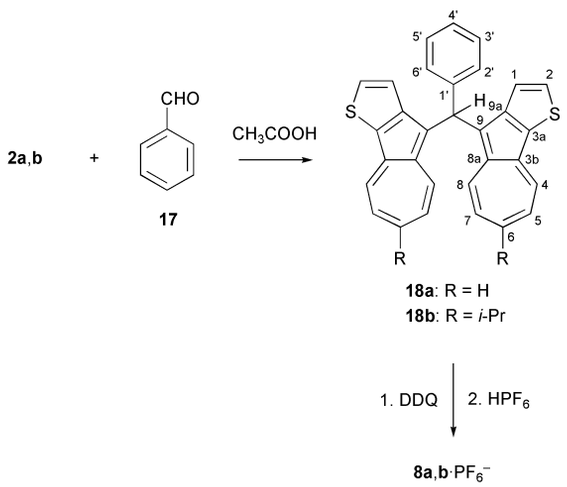

Scheme 3

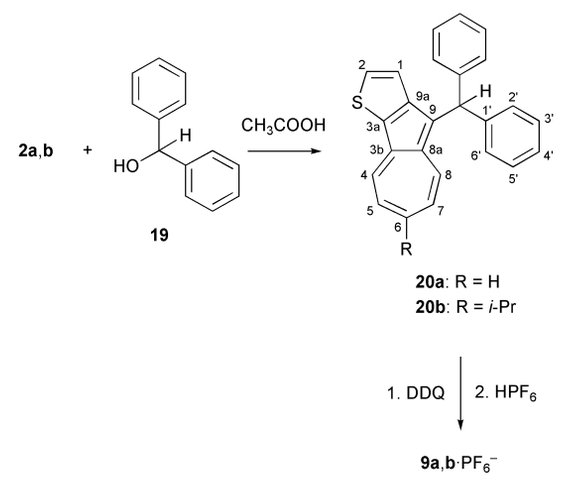

Scheme 4

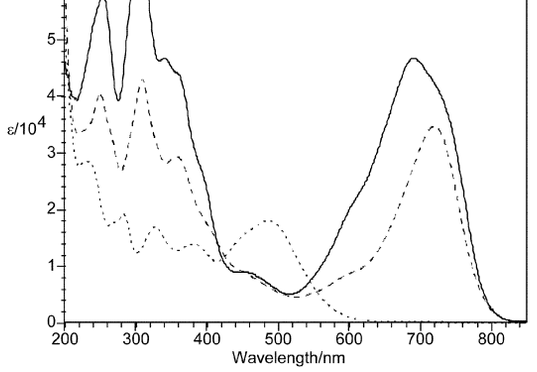

Fig. 1 UV–vis spectra of **7a**·PF_6^- (solid line), **8a**·PF_6^- (broken line), and **9a**·PF_6^- (dotted line) in acetonitrile.

expected by the extension of the π-system, the strong absorption of **7a**,**b**·PF_6^- and **8a**,**b**·PF_6^- in the visible region exhibited an appreciable bathochromic shift by 77–95 nm, respectively, compared with those of **4a**·PF_6^- (614 nm) and **5a**·PF_6^- (639 nm).[9d] In contrast to the bathochromic shift, the absorption of **9a**,**b**·PF_6^- in the visible region showed a slight hypsochromic shift, compared with that of **6a**·PF_6^- (487 nm).[9d]

The methine protons of **16a**,**b**, **18a**,**b** and **20a**,**b** were observed at a slight downfield location on the ^{1}H NMR spectra compared with those of tri(1-azulenyl)methane and its related derivatives. These signals disappeared on the ^{1}H NMR spectra of the hexafluorophosphates **7a**,**b**·PF_6^-, **8a**,**b**·PF_6^- and **9a**,**b**·PF_6^-. Thus, the ^{1}H NMR spectra were also indicative of the cationic structures of these compounds. The central cationic carbons (^{13}C NMR) in **7a**,**b** and **8a**,**b** (**7a**; 148.3 and 148.1, **7b**; 147.9 and 147.5, **8a**; 158.3 and **8b**; 157.8 ppm) were observed at a rather upfield location compared with those of the corresponding cations **4a** and **5a** (157.4 and 165.5 ppm, respectively).[9d] In contrast to the upfield shift, the chemical shift of **9a**,**b** (168.5 and 165.8 ppm, respectively) was comparable with that of mono(1-azulenyl)diphenylmethyl cation **6c** (168.6 ppm).[9d]

The bonding situation of these compounds was examined by comparing the ^3J(H,H) values on the ^{1}H NMR spectra, since a correlation has been shown between these values and the C–C bond distances in the seven-membered ring of azulene.[6,8] Table 2 contains the ^3J(H,H) values in the seven-membered rings of **16a**,**b**, **18a**,**b** and **20a**,**b**. As expected, the ^3J(H,H) values of **16a**, **18a** and **20a** exhibit an alternating pattern of 8.8 Hz across formal C–C bonds and 10.5 Hz across formal C=C bonds. In the 6-isopropyl derivatives **16b**, **18b** and **20b**, the coupling constants slightly increased compared with those of **16a**, **18a** and **20a**: 9.3–9.5 Hz [^3J(4,5)] for the long bonds and 11.0–11.1 Hz [^3J(7,8)] for the short ones. These values are close to those of 6-isopropylazuleno[1,2-*b*]thiophene (**2b**), which has ^3J(H,H) values of 9.3 Hz and 10.8 Hz, respectively. The divergent vicinal coupling constants observed for the seven-membered ring protons on the ^{1}H NMR spectra indicate the existence of a significant bond-length alternation in the azuleno[1,2-*b*]thiophene moiety in analogy with azuleno[1,2-*b*]-thiophene (**2a**,**b**) itself.

^{1}H NMR spectra were also employed for the analysis of the bonding situation in the cations **7a**, **8a** and **9a**. At room temperature, the ^{1}H NMR spectrum of tris[9-(azuleno[1,2-*b*]thienyl)]-methyl cation **7a** consists of four sets of 9-substituted azuleno-[1,2-*b*]thiophene ring-protons with a ratio of *ca.* 1 : 1 : 1 : 1.1 (indicated as a, b, c and d at the 1-H positions in Fig. 2a). The ^{1}H NMR spectrum exhibits the existence of the two isomeric propeller conformations (***7A*** and ***7B***) excluding enantiomeric forms as illustrated in Fig. 3.[9d] Conformer ***7A*** has C_3 symmetry (symmetrical propeller) and has three equivalent 9-azuleno[1,2-*b*]thienyl groups. In contrast to ***7A***, conformer ***7B*** has C_1 symmetry (unsymmetrical propeller) and has three nonequivalent 9-azuleno[1,2-*b*]thienyl groups. Therefore, the three lower-field resonances (a, b and c) correspond to those of

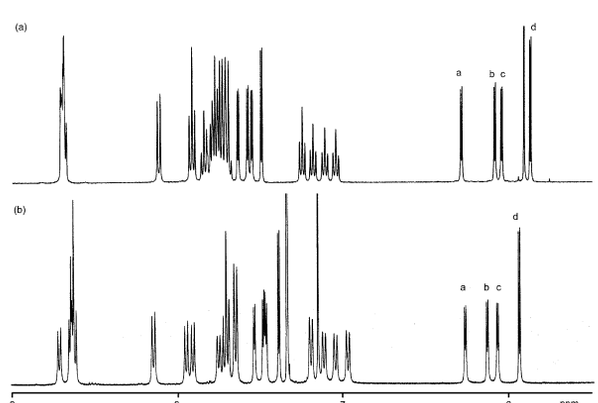

Fig. 2 ^{1}H NMR spectra (600 MHz) of (a) **7a**·PF_6^- in tetrachloroethane-d_2 and (b) **7b**·PF_6^- in C_6D_6–$CDCl_3$ (1 : 30) at the aromatic region.

Table 2 The divergences of the vicinal coupling constants ($\Delta J = {}^3J(7,8) - {}^3J(4,5)$) in **2a**,**b**, the cations **7a**,**b**, **8a**,**b** and **9a**,**b**, and their methane derivatives **16a**,**b**, **18a**,**b** and **20a**,**b**

Cation	Solvent	Conformation	$^3J(7,8)$	$^3J(4,5)$	ΔJ/Hz
2a [a]	$CDCl_3$		10.4	8.8	1.6
2b	$CDCl_3$		10.8	9.3	1.5
16a	50% $CDCl_3$–CS_2		10.5	8.8	1.7
16b	50% $CDCl_3$–CS_2		11.0	9.5	1.5
18a	50% $CDCl_3$–CS_2		10.5	8.8	1.7
18b	$CDCl_3$		11.1	9.3	1.8
20a	$CDCl_3$		10.5	8.8	1.7
20b	$CDCl_3$		11.1	9.3	1.8
7a	$(CDCl_2)_2$	***7A***	10.2	[b]	[b]
		7B	[b]	[b]	[b]
			[b]	[b]	[b]
			[b]	[b]	[b]
7b	C_6D_6 : $CDCl_3$ = 1 : 30	***7A***	10.6	9.9	0.7
		7B	10.8	10.0	0.8
			10.7	9.9	0.8
			10.6	[b]	[b]
8a	$(CDCl_2)_2$		10.1	[b]	[b]
8b	CD_2Cl_2		10.7	10.3	0.4
9a	$CDCl_3$		9.8	9.9	−0.1
9b	$CDCl_3$		10.4	10.6	−0.2

[a] Reported values in reference 3. [b] Vicinal coupling constants could not be obtained due to the low peak separation.

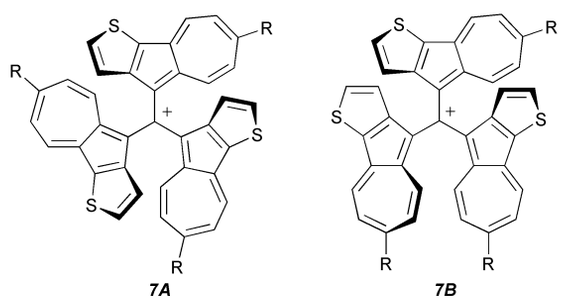

Fig. 3 Presumed conformational isomers for **7**.

7B, while the more intense peak (d) is assigned to those of ***7A***. Unfortunately, the time-averaged ^{1}H NMR spectra of the cation **7a** could not be obtained even by heating at 100 °C in tetrachloroethane-d_2. These phenomena hampered the unequivocal analysis of the vicinal coupling constants of the cation **7a** in the seven-membered ring.

In the case of bis[9-(azuleno[1,2-*b*]thienyl)]methyl cation **8a**, some line broadening was observed on the ^{1}H NMR at room temperature attributed to the conformational interconversion. It is possible for **8a** to exhibit the three isomeric propeller conformations (***8A***, ***8B*** and ***8C***) excluding enantiomeric forms, which are illustrated in Fig. 4.[9d] In spite of the stereoisomerism, the time-averaged ^{1}H NMR spectra of the cation **8a** was obtained on warming the sample at 50 °C in tetrachloroethane-d_2. The relatively low isomerization barrier of **8a** compared with that of **7a** should be attributed to changing the isomerization pathway depending on the steric crowding around the cationic carbon.[9f] However, the charge-transfer interaction between adjacent thiophene and azulene rings might contribute to the relatively high isomerization barrier of **7a**.

At room temperature the NMR of mono[9-(azuleno[1,2-*b*]thienyl)]methyl cation **9a** exhibited two sets of phenyl proton signals with equal intensities and single 9-azuleno[1,2-*b*]thienyl proton signals in the aromatic region. The observed two-phenyl proton signals correspond to the restricted rotation of the azuleno[1,2-*b*]thiophene ring. Only the two *o*-phenyl proton signals indicate the rapid rotation of the two-phenyl groups in the case of **9a**.

Table 2 summarizes the ^3J(H,H) values in the seven-membered rings of the cations **7a**, **8a** and **9a**, which were determined using 500 MHz and/or 600 MHz ^{1}H NMR apparatus. These cations showed a slightly smaller $^3J(7,8)$ values: 10.2

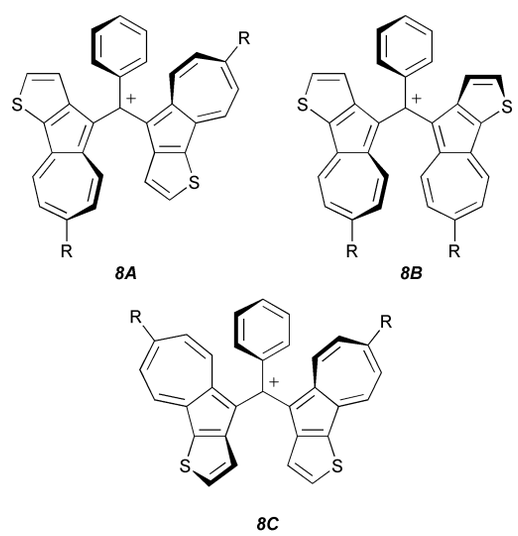

Fig. 4 Presumed conformational isomers for **8**.

Hz in **7a**, 10.1 Hz in **8a** and 9.8 Hz in **9a**, compared to 10.5 Hz in the corresponding methane derivatives **16a**, **18a** and **20a**. However, the $^3J(4,5)$ values of these cations, except for the $^3J(4,5)$ value of **9a** (9.9 Hz), could not be obtained due to the low peak separation even with the use of such high field apparatus. Therefore, it was not possible to resolve the bonding situation within a series of carbocations utilizing the cations **7a**, **8a** and **9a**.

As an alternative, we investigated the ^{1}H NMR of 6-isopropyl derivatives **7b**, **8b** and **9b**, which would enable us to analyze both the $^3J(4,5)$ and $^3J(7,8)$ values within a series of carbocations (Table 2). The ^{1}H NMR spectrum of **7b** in the aromatic region in C_6D_6–$CDCl_3$ (1 : 30) is shown in Fig. 2b. Addition of a small amount of C_6D_6 to $CDCl_3$ increased the peak separation in the aromatic region in the case of **7b**. The NMR spectrum exhibits an unambiguous difference in the coupling constants between $^3J(4,5)$ and $^3J(7,8)$ (ΔJ = 0.7–0.8 Hz), although the difference is rather smaller than that of the corresponding methane derivative **16b** (ΔJ = 1.5 Hz). These results indicate that a substantial degree of bond-length alternation still remains around the perimeter in the cation **7b**, although a trend towards bond equalization is apparent.

The ^{1}H NMR spectrum of the cation **8b** indicates a considerably small difference in the vicinal coupling constants, ΔJ =

Table 3 Computed bond lengths (Å) in **2a** and the cations **7a**, **8a** and **9a**

Cation	Conformation	7,8-Bond	4,5-Bond	Relative heat of formation/kJ mol^{-1}
2a		1.35	1.42	—
7a	***7A***	1.37[a]	1.40[a]	2.0
	7B	1.37[a]	1.40[a]	0.0
8a	***8A***	1.38[a]	1.40[a]	0.9
	8B	1.38[a]	1.40[a]	4.8
	8C	1.38[a]	1.39[a]	0.0
9a		1.40	1.38	—

[a] Average values of three or two independent 7,8-bonds or 4,5-bonds in the conformers.

0.4 Hz, as compared with those in the cation **7b**. Thus, it is concluded that the bond-length alternation in **8b** decreases considerably, although slight alternation still remains.

Although there is a clear variation in the ^3J(H,H) values for the cations **7b** and **8b**, the cation **9b** showed nearly equal ^3J(H,H) values (10.4 and 10.6 Hz) for the seven-membered ring protons in analogy with those of **9a**. The nearly equal ^3J(H,H) values of **9a**,**b** exhibit the azulenium ion character in the azulene core. However, the slightly larger ^3J(4,5) values compared with the ^3J(7,8) values in the case of **9a**,**b** suggest a change in the alternating pattern during the bond-length equalization.

The azulenium ion character in these molecules could also be concluded by the chemical shift of the seven-membered ring protons. The average chemical shift of the protons at the seven-membered ring of **9b** (δ_{av} = 8.30 ppm) is larger than that of **7b** [δ_{av}(conformer ***A***) = 7.92 ppm and δ_{av}(conformer ***B***) = 7.81 ppm] and **8b** (δ_{av} = 7.95 ppm). These facts also indicate that the contribution of the azulenium ion character was increased by the decrease of azulene rings in analogy with the results on the ^3J(H,H) values. Consideration of the average chemical shift at the seven-membered ring on the ^{13}C NMR spectra also led to the same conclusion: **7a** (δ_{av} = 139.0 ppm), **7b** (δ_{av} = 141.3 ppm),[12] **8a** (δ_{av} = 141.1 ppm), **8b** (δ_{av} = 143.9 ppm), **9a** (δ_{av} = 146.8 ppm) and **9b** (δ_{av} = 149.8 ppm).

Semi-emprical MO calculations of azuleno[1,2-*b*]thiophene (**2a**) using the MOPAC PM3 method[13] exhibited long 4,5- (1.42 Å) and short 7,8-bonds (1.35 Å) in analogy with the corresponding long (1.45 Å) and short (1.27 Å) bonds observed in the crystal structure.[7] The rather large difference between the calculated and observed bond lengths should be attributable to the disordered structure of **2a** in the X-ray crystal analysis. Table 3 summarizes the calculated 4,5- and 7,8-bond lengths and relative heats of formation of each conformational isomer of the cations **7a**, **8a** and **9a** calculated by the PM3 method. The most stable stereoisomers of **7a** and **8a** are conformers ***7B*** and ***8C***, respectively, on consideration of the calculated relative heats of formation. The calculation of the cation **7a** exhibits an unequivocal difference in the lengths between 4,5- and 7,8-bonds, although the difference is rather smaller than that of azuleno[1,2-*b*]thiophene (**2a**). The calculation of the cation **8a** indicates a considerably small difference in the lengths between the 4,5- and 7,8-bonds, as compared with that in the cation **7a**. In contrast to the results of **7a** and **8a**, the calculation of the cation **9a** showed a slightly longer 4,5-bond compared with the 7,8-bond in analogy with the results on the slightly larger ^3J(4,5) value than the ^3J(7,8) value of the cation **9a**. These results complement the conclusion obtained by the analysis of ^3J(H,H) values in the cations **7a**, **8a** and **9a**.

The crystal structure of **2b** and the cation **9b** were determined by X-ray diffraction analyses.‡ Suitable crystals of **2b** for X-ray structure determination were obtained by recrystallization from hexane as green needles. The molecule **2b** crystallizes in a monoclinic cell, space group $P2_1/c$ (#14) and Z = 4. An ORTEP drawing of the molecule **2b** is shown in the ESI†. In contrast to the disordered structure of **2a**, the structure of **2b** was obtained with good accuracy. The molecule **2b** exhibits a highly planar framework within 0.022(2) Å from the least-squares plane. The long 4,5- [1.409(2) Å] and short 7,8-bonds [1.377(2) Å] in **2b**, in the crystalline state, show that the unequivocal bond-length alternation is induced by the fusion of the thiophene ring to the azulene skeleton. These lengths were reproduced as the long 4,5- (1.42 Å) and short 7,8-bonds (1.35 Å) by the MOPAC PM3 calculation of **2b** as similar to that of **2a**. As expected, the bond-length alternation in **2b** is slightly smaller than that of 9-phenylbenz[*a*]azulene (**1b**), in which the long 5,6- and short 8,9-bond lengths are observed as 1.422 Å and 1.373 Å, respectively, by X-ray crystallographic analysis.[6] The long 3b,8a-bond [1.501(2) Å], which bridges the azulene system, exhibits the contribution of 10π peripheral delocalization, although the bond localization is apparent in the peripheral bonds. Alternatively, the relatively short 3a,9a-bond [1.401(2) Å] shows that the contribution of 14π peripheral delocalization involving the thiophene ring is less effective than the 10π peripheral delocalization.

Suitable crystals of **9b**·PF_6^- for the X-ray structure determination were obtained by recrystallization from an acetonitrile–diethyl ether–hexane solvent in the presence of excess DDQ. In spite of many efforts, single crystals of the other cations could not be obtained. The cation **9b** crystallized in a monoclinic cell, space group $P2_1/c$ (#14) and Z = 4, with PF_6^- counter anion and DDQ molecule in a ratio of 1 : 1 : 1. The structure of **9b** was obtained with good accuracy although hexafluorophosphate and DDQ molecules are disordered in the crystal structure. An ORTEP drawing and the crystal structure of **9b** are presented in the ESI†.

The azuleno[1,2-*b*]thiophene moiety in **9b** has also an almost planar structure within 0.103(2) Å from the least-squares plane. The observed and calculated values of the bond lengths in **9b** are summarized in Figs. 5a and 5b, respectively. The analysis revealed that the positive charge on the C-α carbon (central cationic carbon) induced the bond-length equalization by the azulenium ion substructure ***9A*** (Chart 4). The slightly longer 7,8-bond [1.395(3) Å] compared with the 4,5-bond [1.376(3) Å] is in accordance with those suggested by the ^3J(H,H) values in the ^{1}H NMR data. The change of the alternating pattern during the bond equalization in **9b** could be attributed to unequal charge distribution in the seven-membered ring.

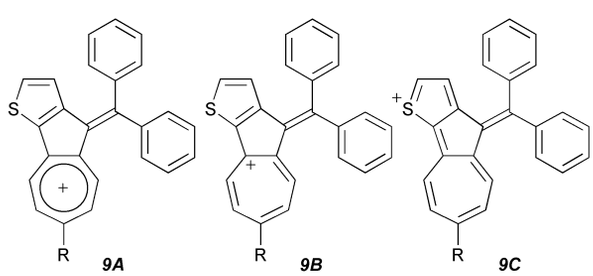

Chart 4

‡ CCDC reference numbers 205749 for **9b** and 205750 for **2b**. See http://www.rsc.org/suppdata/ob/b3/b302688d/ for crystallographic files in CIF or other electronic format.

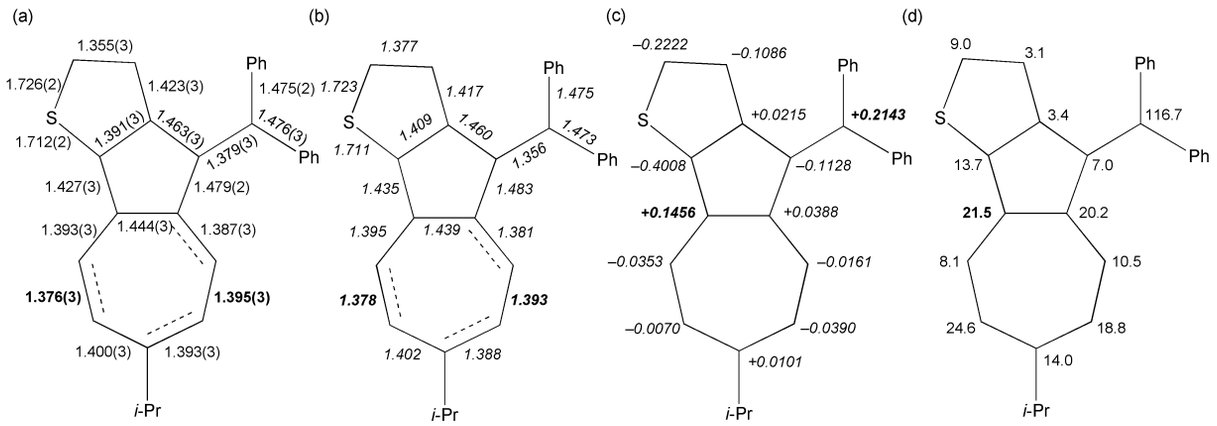

Fig. 5 (a) Observed bond lengths (Å) (X-ray analyses), (b) calculated bond lengths (Å) and (c) net atomic charges of **9b** (MOPAC PM3 method), and (d) $\Delta\delta$ ppm values between the ^{13}C NMR chemical shifts of **9b** and those of the corresponding methane derivative **20b**.

The net atomic charges of **9b** calculated by the MOPAC PM3 method are shown in Fig. 5c. The results exhibit two highly positively charged carbons [C-α and C-3b carbons]. Contribution of the resonance form ***9B***, within the resonance forms derived from ***9A***, should contribute to changing the alternating pattern in the seven-membered ring of **9b**. The relatively high charge distribution on the C-3b carbon corresponds to the relatively large $\Delta\delta$ ppm value (21.5 ppm) between the ^{13}C NMR chemical shift of **9b** and that of the corresponding methane derivative **16b** (Fig. 5d). The natural resonance form ***9C*** involving a positive charge on the sulfur atom is less effective in the case of **9b**, because a significant change in the bond lengths of the thiophene ring compared to those of **2b** was not observed. Several crystal structures of azulenylmethyl cations have been reported.[14] A similar trend in the seven-membered ring has also been found by the X-ray analysis of [4-(dimethylamino)phenyl]-(3-guaiazulenyl)methylium tetrafluoroborate.[14d]

The correlation between the ^3J(H,H) values and the C–C bond distances in the seven-membered rings of **2b** and **9b** together with that between the values and the calculated C–C bond lengths of **2b**, **7a**, **8a** and **9b** is shown in Fig. 6. The trend shows that the reduction of bond-length alternation can be reasonably estimated by ^3J(H,H) values, although the correlation is rough.

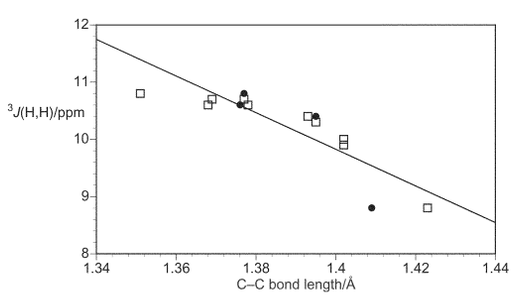

Fig. 6 Correlation between the ^3J(H,H) values and the observed C–C bond distances (X-ray analyses) of **2b** and **9b** (●) and the calculated C–C bond distances (MOPAC PM3 method) of **2b**, **7b**, **8b** and **9b** (□) in the seven-membered ring. In the case of **7b** and **8b**, calculated bond distances of **7a** and **8a** are plotted, since **2a**,**b** and **9a**,**b** did not show significant differences in the calculated C–C bond distances.

As a measure of thermodynamic stability, the pK_R^+ values of **7a**,**b**, **8a**,**b** and **9a**,**b** were determined spectrophotometrically as described in the experimental section.[15] The pK_R^+ scales stand for the carbocation in aqueous solution (pK_R^+ = −log K_R^+). The K_R^+ scale is defined as the equilibrium constant for the reaction of a carbocation with a water molecule (K_R^+ = [ROH][H_3O^+]/[R^+]). Therefore, the larger pK_R^+ index indicates a smaller K_R^+ value and, in turn, a higher stability of the carbocation. The values of **7a**,**b**, **8a**,**b** and **9a**,**b** and those of **4a**, **5a** and **6a**[9d] are summarized in Table 4.

Table 4 pK_R^+ values[a] **7a**,**b**, **8a**,**b** and **9a**,**b** together with those of **4a**, **5a** and **6a**

Cation	pK_R^+	Cation	pK_R^+
7a	11.6 ± 0.1 (81%) [b]	**9b**	5.5 ± 0.1 (41%) [b]
7b	13.8 ± 0.1 (47%) [b]	**4a**	11.3
8a	10.7 ± 0.1 (22%) [b]	**5a**	10.5
8b	11.7 ± 0.1 (46%) [b]	**6a**	3.0
9a	4.4 ± 0.1 (99%) [b]		

[a] The pK_R^+ values were determined by spectrophotomerically at 25 °C in a buffered solution prepared in 50% aqueous MeCN. [b] Regenerated absorption maxima (%) of the cations in visible region by the immediate acidification of the alkaline solution with HCl after the pK_R^+ measurement were shown in parentheses.

As expected by the extension of the π-system stabilizing the carbocation, the pK_R^+ values of **7a**, **8a** and **9a** were slightly increased by 0.2–1.4 pK units compared to those of **4a**, **5a** and **6a**. The larger pK_R^+ values indicate a higher degree of thermodynamic stability of these cations compared to those of **4a**, **5a** and **6a**. The pK_R^+ values of the isopropyl derivatives **7b**, **8b** and **9b** are higher by 1.0–2.2 pK units than those of the parent cations **7a**, **8a** and **9a**. Stabilization with the 6-isopropyl substituents on each azuleno[1,2-*b*]thiophene ring is in analogy with our previous results on the stabilization of tri(1-azulenyl)methyl cations with 3- and/or 6-*tert*-butyl substituents on each azulene ring.[9d] The effect of the substituents would be attributable to their steric and also their inductive electronic effects induced by C–C hyperconjugation at the positively charged C-6 carbon.

The redox potentials (V *vs.* Ag/Ag^+) of **7a**,**b**, **8a**,**b** and **9a**,**b** were determined by CV. The CV waves of compounds **7a**, **8a** and **9a**, redox details of compounds **7a**,**b**, **8a**,**b** and **9a**,**b** along with those of **4a**, **5a** and **6a**[9d] are shown in the ESI †. The reduction of **7a**, **8a** and **9a** showed an irreversible wave at −0.75, −0.67 and −0.53 V, respectively. These reduction potentials are in the potential range comparable with those of **4a**, **5a** and **6a** in spite of the condensation of the thiophene rings. 6-Isopropyl substituents on each azuleno[1,2-*b*]thienyl group slightly increased the reversibility of the reduction upon CV. The reduction of **7b** showed a reversible wave at −0.81 V and an irreversible wave at −1.51 V upon the CV. These two waves are ascribed to the formation of a radical and an anion, respectively. The more negative reduction potentials of the 6-isopropyl derivatives **7b**, **8b** and **9b**, compared to those of **7a**, **8a** and **9a**, correspond to the increase of the electrochemical stability by the isopropyl substituents in analogy with the results on the pK_R^+ measurements. Peak broadening arising from stereoisomerism was not observed in these cases.

The electrochemical oxidation of **7a**,**b** exhibited voltammograms characterized by barely separated reversible waves at

0.75–0.91 V. The oxidation process is due to generation of a tricationic species by the oxidation of two azuleno[1,2-*b*]-thiophene moieties. These oxidation potentials are less positive than those of **4a** by 0.16–0.23 V. In the oxidation of **7a**,**b**, irreversible waves were observed at 1.42 and 1.44 V, respectively, upon CV. The oxidation of **8a**,**b** showed reversible waves at 0.85 and 0.82 V, respectively and irreversible waves both at 1.37 V. More positive oxidation potentials observed by the oxidation of **9a**,**b** are ascribed to the formation of a dication radical by the oxidation of an azuleno[1,2-*b*]thiophene ring.

Conclusions

The titled stable tris-, bis- and mono[9-(azuleno[1,2-*b*]thienyl)]-methyl cations and their 6-isopropyl derivatives **7a**,**b**, **8a**,**b** and **9a**,**b** were prepared by the hydride abstraction reaction of the corresponding methane derivatives **16a**,**b**, **18a**,**b** and **20a**,**b**. The seven-membered rings of **16a**,**b**, **18a**,**b** and **20a**,**b** exhibit bond-length alternation in analogy with azuleno[1,2-*b*]thiophene itself. The cations **7a**,**b** and **8a**,**b** also exhibited the alternating C–C bond lengths in the seven-membered ring, although the reduction of the bond-length alternation is observed. The cations **9a**,**b** indicate that a delocalized tropylium substructure is developed around the seven-membered ring. From these results on the analysis of the ^3J(H,H) values, it would be concluded that the bond alternation in the fused azulene systems does not disappear all at once with the connection of a methyl cation, but decreases continuously with the decrease of the number of azulene rings. The X-ray crystal analysis of **2b** and **9b** revealed the bond-length equalization. The stabilities examined by pK_R^+ values and redox potentials were not significantly affected by the fused thiophene ring, although the fusion causes the bond-length alternation in the azulene systems.

Experimental

General

Melting points were determined on a Yanagimoto micro melting point apparatus MP-S3 and are uncorrected. Mass spectra were obtained with a JEOL HX-110 or a Hitachi M-2500 instrument, usually at 70 eV. IR and UV spectra were measured on a Shimadzu FTIR-8100M and a Hitachi U-3410 spectrophotometer, respectively. ^{1}H NMR spectra (^{13}C NMR spectra) were recorded on a JEOL GSX 400 at 400 MHz (100 MHz), a JEOL JNM A500 at 500 MHz (125 MHz) or a Bruker AM 600 spectrometer at 600 MHz (150 MHz). Gel permeation chromatography (GPC) purification was performed on a TSKgel G2000H$_6$. Voltammetry measurements were carried out with a BAS100B/W electrochemical workstation equipped with Pt working and auxiliary electrodes, a reference electrode formed from Ag/AgNO$_3$ (0.01 M, 1 M = 1 mol dm^{-3}) and tetraethylammonium perchlorate (TEAP) as a supporting electrolyte, at the scan rate of 100 mV s^{-1}. Elemental analyses were performed at the Instrumental Analysis Center of Chemistry, Faculty of Science, Tohoku University.

Methyl 1,2-dihydro-6-isopropyl-9-(azuleno[1,2-*b*]thiophene)-carboxylate 12

A mixture of the enamines **11a**,**b** was prepared by the reaction of tetrahydrothiophene-3-one (25.3 g, 248 mmol) with morpholine (42.7 g, 490 mmol) in refluxing benzene (200 ml). A solution of **10** (15.3 g, 62.1 mmol) and a mixture of the enamines **11a**,**b** in abs. ethanol (750 ml) was refluxed for 4 days under an Ar atmosphere. The reaction mixture was poured into water and extracted with toluene. The organic layer was washed with brine and water, dried with MgSO$_4$ and concentrated under reduced pressure. The residue was purified by column chromatography on silica gel with toluene to afford **12** (8.36 g, 47%) as green plates and methyl 1,3-dihydro-6-isopropyl-9-(azuleno[1,2-*c*]thiophene)carboxylate (**13**) (2.22 g, 12%) as purple powder.

For **12**. Mp 113.6–114.0 °C decomp. (from MeOH) (Found: C, 71.2; H, 6.4; S, 10.95. Calc. for $C_{17}H_{18}SO_2$: C, 71.3; H 6.3; S, 11.2%); ν_{max} (KBr disk)/cm^{-1} 2957, 1682 (C=O), 1443, 1412, 1219 and 1073 cm^{-1}; λ_{max} (CH_2Cl_2)/nm 270 (log ε 4.46), 326 (4.57), 333 sh (4.56), 412 sh (3.69), 432 (3.76), 593 (2.90), 641 sh (2.82) and 721 sh (2.28); *m*/*z* (EI) 286 (M$^+$, 100%).

For **13**. Mp 121.5–122.0 °C (from MeOH) (Found: C, 71.2; H, 6.6; S; 11.0. Calc. for $C_{17}H_{18}SO_2$: C, 71.3; H 6.3; S, 11.2%); ν_{max} (KBr disk)/cm^{-1} 1692 (C=O), 1445, 1420, 1206 and 1092; λ_{max} (CH_2Cl_2)/nm 237 (log ε 4.28), 258 sh (3.89), 305 (4.64), 311 (4.65), 353 (3.81), 366 (3.79), 386 (3.76), 435 sh (2.34), 525 (2.71), 559 sh (2.64) and 618 sh (2.12); *m*/*z* (EI) 286 (M$^+$, 100%), 271 (20), 254 (M$^+$ − MeOH, 32) and 243 (M$^+$ − *i*Pr, 24).

Methyl 6-isopropyl-9-(azuleno[1,2-*b*]thiophene)carboxylate 14

A mixture of **12** (8.36 g, 29.2 mmol) and DDQ (8.29 g, 36.5 mmol) in dry toluene (150 ml) was stirred at 80 °C for 5 h. After the solvent was removed under reduced pressure, the residue was purified by column chromatography on silica gel with toluene to afford **14** (7.31 g, 88%) as greenish blue plates, mp 139.5–141.0 °C decomp. (from MeOH) (Found: C, 71.9; H, 5.7; S, 11.0. Calc. for $C_{17}H_{16}SO_2$: C, 71.8; H 5.7; S, 11.3%); ν_{max} (KBr disk)/cm^{-1} 1680 (C=O), 1460, 1408, 1204 and 1090; λ_{max} (CH_2Cl_2)/nm 235 (log ε 4.23), 279 sh (4.13), 291 (4.23), 331 (4.66), 343 (4.72), 377 sh (3.83), 395 (3.99), 412 sh (3.72), 518 sh (2.47), 564 (2.63), 604 sh (2.58) and 664 sh (2.13); *m*/*z* (EI) 284 (M$^+$, 100%) and 253 (M$^+$ − OMe, 29).

6-Isopropylazuleno[1,2-*b*]thiophene 2b

A mixture of **14** (2.00 g, 7.03 mmol) and 100% phosphoric acid, which was freshly prepared using 85% phosphoric acid (140 g) and phosphorous pentaoxide (55 g), was heated at 90 °C for 30 min with occasional stirring with a glass rod. After cooling the reaction mixture, the mixture was poured into water and extracted with toluene. The organic layer was washed with water and 5% NaHCO$_3$ solution, dried with MgSO$_4$ and concentrated under reduced pressure. The residue was purified by column chromatography on silica gel with 20% toluene–hexane to afford **2b** (1.51 g, 95%) as greenish blue plates, mp 89.6–90.4 °C decomp. (from MeOH) (Found: C, 79.7; H, 6.3; S, 14.1. Calc. for $C_{15}H_{14}S$: C, 79.6; H 6.2; S, 14.2%); ν_{max} (KBr disk)/cm^{-1} 1578, 1397, 833 and 662; λ_{max} (CH_2Cl_2)/nm 241 sh (log ε 4.00), 286 (4.48), 312 (4.70), 320 (4.68), 363 (3.74), 380 (3.78), 399 (3.70), 552 sh (2.55), 607 (2.71), 650 (2.66) and 736 sh (2.22); *m*/*z* (EI) 226 (M$^+$, 100%) and 211 (M$^+$ − Me, 34).

9-(Azuleno[1,2-*b*]thiophene)carbaldehyde 15a

A solution of POCl$_3$ (1.84 g, 12.0 mmol) in DMF (5 ml) was slowly added at room temperature to a solution of **2a** (1.84 g, 10.0 mmol) in DMF (50 ml). The resulting solution was stirred at the same temperature for 16 h. The reaction mixture was poured into water, made alkaline with saturated K$_2$CO$_3$ and then extracted with toluene. The organic layer was washed with water, dried with MgSO$_4$ and concentrated under reduced pressure. Purification of the residue by column chromatography on silica gel with CH_2Cl_2 gave **15a** (1.97 g, 93%) as deep blue prisms, mp 79.9–80.5 °C (from toluene) (Found: C, 73.6; H, 3.95; S, 14.9. Calc. for $C_{13}H_8SO$: C, 73.6; H 3.8; S, 15.1%); ν_{max} (KBr disk)/cm^{-1} 1626 (C=O), 1503, 1455, 1364 and 752; λ_{max} (CH_2Cl_2)/nm 235 (log ε 4.21), 293 (4.25), 336 sh (4.53), 349 (4.62), 399 (3.94), 418 sh (3.87), 532 sh (2.48), 572 (2.58), 618 sh (2.50) and 687 sh (1.96); *m*/*z* (EI) 212 (M$^+$, 100%), 211 (67) and 139 (23).

6-Isopropyl-9-(azuleno[1,2-*b*]thiophene)carbaldehyde 15b

The same procedure used for the preparation of **15a** was adopted. The reaction of **2b** (113 mg, 0.499 mmol) in DMF

(3 ml) with $POCl_3$ (92 mg, 0.60 mmol) in DMF (3 ml) afforded **15b** (109 mg, 86%) as dark green plates, mp 73.2–73.9 °C decomp. (from hexane) (Found: C, 75.3; H, 5.7; S, 12.7. Calc. for $C_{16}H_{14}SO$: C, 75.6; H 5.55; S, 12.6%); ν_{max} (KBr disk)/cm^{-1} 1630 (C=O), 1399, 1368 and 793; λ_{max} (CH_2Cl_2)/nm 242 sh (log ε 4.18), 281 sh (4.17), 295 (4.26), 339 sh (4.56), 353 (4.64), 400 (4.01), 415 sh (3.90), 513 sh (2.58), 553 (2.66), 597 sh (2.57), 656 sh (2.23) and 703 (2.06); *m*/*z* (EI) 254 (M^+, 100%) and 253 (39).

Tris[9-(azuleno[1,2-*b*]thienyl)]methane 16a

A solution of **2a** (1.29 g, 7.00 mmol) and **15a** (743 mg, 3.50 mmol) in acetic acid (40 ml) was stirred at room temperature for 25 days under an Ar atmosphere. The solvent was removed under reduced pressure. The residue was diluted with CH_2Cl_2 and neutralized with $NaHCO_3$ solution. The organic layer was washed with water, dried with $MgSO_4$ and concentrated under reduced pressure. The residue was purified by column chromatography on silica gel with toluene to afford **16a** (1.49 g, 76%) as green powder, mp 263.2–270.0 °C decomp. (from toluene) (Found: C, 78.7; H, 4.15, S, 16.9. Calc. for $C_{37}H_{22}S_3$: C, 79.0; H 3.9; S, 17.1%); ν_{max} (KBr disk)/cm^{-1} 1574, 1453, 1387 and 745; λ_{max} (CH_2Cl_2)/nm 233 (log ε 4.56), 249 sh (4.47), 286 (4.87), 313 sh (4.99), 319 (5.02), 333 (4.90), 370 (4.11), 389 (4.18), 406 sh (3.87), 596 sh (2.92), 650 (3.07), 704 (3.03) and 793 sh (2.57); *m*/*z* (EI) 562 (M^+, 100%), 561 (37), 380 (33), 379 ($M^+ - C_{12}H_7S$, 31), 378 (35), 377 (49) and 184 ($C_{12}H_8S^+$, 28).

Tris[6-isopropyl-9-(azuleno[1,2-*b*]thienyl)]methane 16b

A solution of **2b** (294 mg, 1.30 mmol) and **15b** (127 mg, 0.499 mmol) in acetic acid (8 ml) was stirred at room temperature for 21 days under an Ar atmosphere. The reaction mixture was diluted with CH_2Cl_2 and neutralized with $NaHCO_3$ solution. The precipitated crystals were collected by filtration. Purification by recrystallization from tetrachloroethane to afford **16b** (144 mg, 42%) as green powder, mp > 300 °C (from toluene) (Found: C, 80.1; H, 6.1; S, 13.85. Calc. for $C_{46}H_{40}S_3$: C, 80.2; H 5.85; S, 14.0%); ν_{max} (KBr disk)/cm^{-1} 2959, 1580, 1460, 1435, 1393 and 831; λ_{max} (CH_2Cl_2)/nm 232 (log ε 4.48), 289 (4.83), 320 (5.02), 336 (4.95), 372 (4.19), 390 (4.24), 410 sh (3.92), 575 sh (2.91), 632 (3.07), 681 (3.04) and 772 sh (2.60); *m*/*z* (EI) 688 (M^+, 100%), 687 (44), 686 (52), 646 (28), 645 ($M^+ - i$Pr, 56), 464 (25), 462 ($M^+ - C_{15}H_{14}S$, 26) and 226 ($C_{15}H_{14}S^+$, 26).

Bis[9-(azuleno[1,2-*b*]thienyl)]phenylmethane 18a

The same procedure used for the preparation of **16a** was adopted. The reaction of **2a** (369 mg, 2.00 mmol) with **17** (214 mg, 2.02 mmol) in acetic acid (10 ml) at room temperature for 4 h and column chromatography on silica gel with toluene afforded **18a** (417 mg, 91%) as green needles, mp 255.3–256.0 °C decomp. (from toluene) (Found: C, 81.7; H, 4.7; S, 13.6. Calc. for $C_{31}H_{20}S_2$: C, 81.5; H 4.4; S, 14.0%); ν_{max} (KBr disk)/cm^{-1} 1574, 1453, 1387, 800, 745, 700 and 677; λ_{max} (CH_2Cl_2)/nm 231 (log ε 4.44), 289 (4.73), 318 (4.88), 332 (4.74), 370 (3.92), 388 (4.00), 407 sh (3.66), 595 sh (2.77), 647 (2.92), 702 (2.87) and 788 sh (2.43); *m*/*z* (EI) 456 (M^+, 100%), 455 (30) and 271 (30).

Bis[6-isopropyl-9-(azuleno[1,2-*b*]thienyl)]phenylmethane 18b

The same procedure used for the preparation of **16a** was adopted. Reaction of **2b** (227 mg, 1.00 mmol) with **17** (168 mg, 1.58 mmol) in acetic acid (5 ml) at room temperature for 3 h and column chromatography on silica gel with 50% toluene–hexane afforded **18b** (223 mg, 82%) as green powder, mp 191.5–192.0 °C decomp. (from ether–hexane) (Found: C, 81.9; H, 6.1; S, 11.4. Calc. for $C_{37}H_{32}S_2$: C, 82.2; H 6.0; S, 11.9%); ν_{max} (KBr disk)/cm^{-1} 2957, 1578, 1460, 1449, 1393, 833 and 743; λ_{max} (CH_2Cl_2)/nm 290 (log ε 4.70), 319 (4.90), 335 (4.78), 371 (3.97), 390 (4.04), 408 sh (3.70), 567 sh (2.71), 630 (2.90), 685 (2.86) and 768 sh (2.41); *m*/*z* (EI) 540 (M^+, 87%), 498 (40), 497 ($M^+ - i$Pr, 100) and 271 (28).

[9-(Azuleno[1,2-*b*]thienyl)]diphenylmethane 20a

The same procedure used for the preparation of **16a** was adopted. Reaction of **2a** (552 mg, 3.00 mmol) with **19** (552 mg, 3.00 mmol) in refluxing acetic acid (15 ml) for 21 h and column chromatography on silica gel with 10% ethyl acetate–hexane and GPC with $CHCl_3$ afforded **20a** (466 mg, 44%) as deep blue prisms, mp 146.8–147.0 °C (from hexane) (Found: C, 85.6; H, 5.3; S, 8.9. Calc. for $C_{25}H_{18}S$: C, 85.7; H 5.2; S, 9.15%); ν_{max} (KBr disk)/cm^{-1} 1574, 1493, 1453, 1387, 758, 743 and 700; λ_{max} (CH_2Cl_2)/nm 231 (log ε 4.20), 292 sh (4.42), 318 (4.65), 330 sh (4.52), 367 (3.62), 385 (3.70), 405 sh (3.27), 584 sh (2.44), 643 (2.61), 701 (2.55) and 785 sh (2.10); *m*/*z* (EI) 350 (M^+, 100%), 274 (20), 273 ($M^+ - C_6H_5$, 96) and 271 (35).

[6-Isopropyl-9-(azuleno[1,2-*b*]thienyl)]diphenylmethane 20b

The same procedure used for the preparation of **16a** was adopted. Reaction of **2b** (99 mg, 0.44 mmol) with **19** (406 mg, 2.20 mmol) in refluxing acetic acid (3 ml) for 2 h and column chromatography on silica gel with 10% toluene–hexane afforded **20b** (70 mg, 41%) as blue powder, mp 197.0–197.5 °C (from hexane) (Found: C, 85.6; H, 6.3; S, 7.95. Calc. for $C_{28}H_{24}S$: C, 85.7; H 6.2; S, 8.2%); ν_{max} (KBr disk)/cm^{-1} 1580, 1460, 1445, 1389, 749 and 702; λ_{max} (CH_2Cl_2)/nm 232 (log ε 4.19), 293 sh (4.45), 319 (4.74), 332 (4.66), 369 (3.76), 387 (3.82), 404 sh (3.50), 515 (2.31), 568 sh (2.52), 623 (2.68), 672 sh (2.64) and 759 sh (2.19); *m*/*z* (EI) 392 (M^+, 100%) and 315 ($M^+ -$ Ph, 65).

Tris[9-(azuleno[1,2-*b*]thienyl)]methylium hexafluorophosphate (7a·PF_6^-)

DDQ (96 mg, 0.42 mmol) was added at room temperature to a solution of **16a** (198 mg, 0.352 mmol) in CH_2Cl_2 (60 ml). After the solution was stirred at the same temperature for 10 min, 60% HPF_6 (3 ml) and water (50 ml) were added to the reaction mixture. The precipitated crystals were removed by filtration. The organic layer was separated, washed with water, dried with $MgSO_4$ and concentrated under reduced pressure. The residue was crystallized from CH_2Cl_2–ether to give **6a**·PF_6^- (215 mg, 86%) as dark purple powder, mp 262.5–264.2 °C decomp. (from CH_3CN–ether) (Found: C, 62.6; H, 3.35; S, 13.5. Calc. for $C_{37}H_{21}S_3 \cdot PF_6$: C, 62.9; H 3.0; S, 13.6%); ν_{max} (KBr disk)/cm^{-1} 1470, 1455, 1406, 1393, 1294, 1281, 839 and 558; λ_{max} (MeCN)/nm 254 (log ε 4.76), 309 (4.83), 341 (4.67), 362 sh (4.64), 393 sh (4.42), 463 sh (3.94), 605 sh (4.32), 691 (4.67) and 733 sh (4.59); *m*/*z* (FAB) 561 ($M^+ - PF_6$).

Tris[6-isopropyl-9-(azuleno[1,2-*b*]thienyl)]methylium hexafluorophosphate (7b·PF_6^-)

The same procedure used for the preparation of **7a**·PF_6^- was adopted. The reaction of **16b** (80 mg, 0.12 mmol) with DDQ (32 mg, 0.14 mmol) in CH_2Cl_2 (10 ml) at room temperature for 20 min and crystallization from CH_3CN–ether afforded **7b**·PF_6^- (73 mg, 75%) as dark green prisms, mp 210.0–211.5 °C decomp. (from CH_2Cl_2–ether) (Found: C, 66.2; H, 4.9; S, 11.7. Calc. for $C_{46}H_{39}S_3 \cdot PF_6$: C, 66.3; H 4.7; S, 11.55%); ν_{max} (KBr disk)/cm^{-1} 1458, 1418, 1393, 1308, 1283, 1267, 1242, 839 and 558; λ_{max} (MeCN)/nm 256 (log ε 4.70), 310 (4.85), 344 (4.70), 361 (4.70), 392 sh (4.52), 450 (4.02), 591 sh (4.23), 686 (4.66) and 709 (4.66); *m*/*z* (FAB) 687 ($M^+ - PF_6$).

Bis[9-(azuleno[1,2-*b*]thienyl)]phenylmethylium hexafluorophosphate (8a·PF_6^-)

The same procedure used for the preparation of **7a**·PF_6^- was adopted. The reaction of **18a** (202 mg, 0.442 mmol) with DDQ (119 mg, 0.524 mmol) in CH_2Cl_2 (30 ml) at room temperature

for 20 min and crystallization from CH_2Cl_2–ether afforded **8a**·PF_6^- (215 mg, 81%) as dark blue powder, mp > 300 °C (from CH_3CN–ether) (Found: C, 61.9; H, 3.4; S, 10.4. Calc. for $C_{31}H_{19}S_2$·PF_6: C, 62.0; H 3.2; S, 10.7%); ν_{max} (KBr disk)/cm^{-1} 1472, 1453, 1393, 1291, 1169, 839 and 558; λ_{max} (MeCN)/nm 248 (log ε 4.61), 309 (4.63), 357 (4.47), 404 sh (4.21), 451 sh (3.95), 594 sh (3.92) and 718 (4.54); *m*/*z* (FAB) 455 ($M^+ - PF_6$).

Bis[6-isopropyl-9-(azuleno[1,2-*b*]thienyl)]phenylmethylium hexafluorophosphate (**8b**·PF_6^-)

The same procedure used for the preparation of **7a**·PF_6^- was adopted. The reaction of **18b** (109 mg, 0.202 mmol) with DDQ (55 mg, 0.24 mmol) in CH_2Cl_2 (18 ml) at room temperature for 25 min and crystallization from CH_2Cl_2–ether afforded **8b**·PF_6^- (87 mg, 63%) as dark green plates, mp 135.2–136.0 °C (from CH_2Cl_2–ether) (Found: C, 65.4; H, 4.5; S, 9.4. Calc. for $C_{37}H_{31}S_2$·PF_6: C, 64.9; H 4.6; S, 9.4%); ν_{max} (KBr disk)/cm^{-1} 1474, 1393, 1281, 1242, 837 and 558; λ_{max} (MeCN)/nm 250 (log ε 4.54), 261 sh (4.50), 312 (4.65), 359 (4.48), 404 sh (4.20), 573 sh (3.83) and 721 (4.46); *m*/*z* (FAB) 539 ($M^+ - PF_6$).

[9-(Azuleno[1,2-*b*]thienyl)]diphenylmethylium hexafluorophosphate (**9a**·PF_6^-)

The same procedure used for the preparation of **7a**·PF_6^- was adopted. The reaction of **20a** (105 mg, 0.300 mmol) with DDQ (81 mg, 0.36 mmol) in CH_2Cl_2 (30 ml) at room temperature for 10 min and crysatllization from CH_2Cl_2–ether afforded **9a**·PF_6^- (122 mg, 82%) as red powder, mp 188.8–190.0 °C decomp. (from CH_3CN–ether) (Found: C, 60.8; H, 3.8; S, 6.7. Calc. for $C_{25}H_{17}S$·PF_6: C, 60.7; H 3.5; S, 6.5%); ν_{max} (KBr disk)/cm^{-1} 1547, 1447, 839 and 558; λ_{max} (MeCN)/nm 230 (log ε 4.46), 269 sh (4.25), 284 (4.29), 327 (4.23), 382 (4.14), 441 sh (4.15) and 486 (4.26); *m*/*z* (FAB) 349 ($M^+ - PF_6$).

[6-Isopropyl-9-(azuleno[1,2-*b*]thienyl)]diphenylmethylium hexafluorophosphate (**9b**·PF_6^-)

The same procedure used for the preparation of **7a**·PF_6^- was adopted. The reaction of **20b** (73 mg, 0.19 mmol) with DDQ (130 mg, 0.573 mmol) in CH_2Cl_2 (8 ml) at room temperature for 20 min and crystallization from CH_3CN–ether afforded **9b**·PF_6^- (95 mg, 95%) as red powder, mp 139.0–140.0 °C decomp. (from CH_2Cl_2–ether) (Found: C, 62.8; H, 4.1; S, 5.9. Calc. for $C_{28}H_{23}S$·PF_6: C, 62.7; H 4.3; S, 5.8%); ν_{max} (KBr disk)/cm^{-1} 1439, 1325, 1175, 837 and 558; λ_{max} (MeCN)/nm 233 (log ε 4.40), 272 sh (4.31), 281 (4.33), 326 (4.17), 387 (4.14) and 481 (4.17); *m*/*z* (FAB) 391 ($M^+ - PF_6$).

The pK_R^+ value

Sample solutions of the hexafluorophosphates **7a**,**b**·PF_6^- and **8b**·PF_6^- were prepared by dissolving 1–2 mg of the hexafluorophosphates in MeCN and a glycine (0.1 M) solution (50 ml) and made up to 100 ml by further adding MeCN; the sample solution with lower acidity was made by further alkalification with 20% aqueous NaOH. For the preparation of a sample solution of the hexafluorophosphates **8a**·PF_6^- and **9a**,**b**·PF_6^-, buffer solutions of slightly different acidities were prepared by mixing CH_3COONa (1 M) and HCl (1 M) for pH 1.0–3.0, CH_3COONa (0.1 M) and CH_3COOH (0.1 M) for pH 3.2–5.0, KH_2PO_4 (0.1 M) and $Na_2B_4O_7$ (0.05 M) for pH 6.0–9.0, $Na_2B_4O_7$ (0.05 M) and Na_2CO_3 (0.05 M) for pH 10.0, and $Na_2B_4O_7$ (0.05 M) and NaOH (0.1 M) for pH 11.0–11.4, in various portions. Each 1 ml portion of the stock solution, prepared by dissolving 2–3 mg of the hexafluorophosphates **8a**·PF_6^- and **9a**,**b**·PF_6^- in MeCN (20 ml), was pipetted out and made up to 10 ml by adding an appropriate buffer solution (5 ml) and MeCN. The pH of each sample was made on a Horiba pH meter F-13 calibrated with standard buffers before use. The observed absorbance at the specific absorption maxima in visible region of the cations **7a**,**b**, **8a**,**b** and **9a**,**b** were plotted against the pH, giving classical titration curves whose midpoints were taken as the pK_R^+ values.

Acknowledgements

The present work was supported by a Grant-in-Aid for Scientific Research (No. 14540486 to S. I.) from the Ministry of Education, Culture, Sports, Science and Technology, Japan.

References and notes

1 (*a*) K.-P. Zeller, Azulene, in *Houben-Weyl; Methoden der Organischen Chemie*, ed. H. Kropf, Georg Thieme, Stuttgart, 4th edn., 1985, vol. V, part 2c, pp. 127–418; (*b*) D. M. Lemal and G. D. J. Goldman, *J. Chem. Educ.*, 1988, **65**, 923–925.
2 (*a*) J. M. Robertson and H. M. M. Shearer, *Nature*, 1956, **177**, 885; (*b*) J. M. Robertson, H. M. M. Shearer, G. A. Sim and D. G. Watson, *Nature*, 1958, **182**, 177–178; (*c*) J. M. Robertson, H. M. Shearer, G. A. Sim and D. G. Watson, *Acta Crystallogr.*, 1962, **15**, 1–8; (*d*) A. W. Hansen, *Acta Crystallogr.*, 1965, **19**, 19–26.
3 K. Fujimori, T. Fujita, K. Yamane, M. Yasunami and K. Takase, *Chem. Lett.*, 1983, 1721–1724.
4 D. J. Bertelli and P. Crews, *Tetrahedron*, 1970, **26**, 4717–4728.
5 T. Morita, T. Nakadate and K. Takase, *Heterocycles*, 1981, **15**, 835–838.
6 M. Bühl, W. Kozminski, A. Linden, D. Nanz, D. Sperandio and H.-J. Hansen, *Helv. Chim. Acta*, 1996, **79**, 837–854.
7 S. Kashino, M. Haisa, K. Fujimori and K. Yamane, *Acta Crystallogr., Sect. B: Struct. Crystallogr. Cryst. Chem.*, 1982, **38**, 2729–2731.
8 Y. Lu, D. M. Lemal and J. P. Jasinski, *J. Am. Chem. Soc.*, 2000, **122**, 2440–2445.
9 (*a*) S. Ito, N. Morita and T. Asao, *Tetrahedron Lett.*, 1991, **32**, 773–776; (*b*) S. Ito, N. Morita and T. Asao, *Tetrahedron Lett.*, 1994, **35**, 751–754; (*c*) S. Ito, N. Morita and T. Asao, *Tetrahedron Lett.*, 1994, **35**, 3723–3726; (*d*) S. Ito, N. Morita and T. Asao, *Bull. Chem. Soc. Jpn.*, 1995, **68**, 1409–1436; (*e*) S. Ito, N. Morita and T. Asao, *Bull. Chem. Soc. Jpn.*, 1995, **68**, 2011–2016; (*f*) S. Ito, N. Morita and T. Asao, *Bull. Chem. Soc. Jpn.*, 1995, **68**, 2639–2648; (*g*) S. Ito, M. Fujita, N. Morita and T. Asao, *Chem. Lett.*, 1995, 475–476; (*h*) S. Ito, M. Fujita, N. Morita and T. Asao, *Bull. Chem. Soc. Jpn.*, 1995, **68**, 3611–3620; (*i*) S. Ito, S. Kikuchi, N. Morita and T. Asao, *Chem. Lett.*, 1996, 175–176; (*j*) S. Ito, H. Kobayashi, S. Kikuchi, N. Morita and T. Asao, *Bull. Chem. Soc. Jpn.*, 1996, **69**, 3225–3237; (*k*) S. Ito, S. Kikuchi, N. Morita and T. Asao, *Bull. Chem. Soc. Jpn.*, 1999, **72**, 839–849; (*l*) S. Ito, S. Kikuchi, N. Morita and T. Asao, *J. Org. Chem.*, 1999, **64**, 5815–5821.
10 K. Yamamura, N. Kusuhara, Y. Houda, M. Sasabe, H. Takagi and M. Hashimoto, *Tetrahedron Lett.*, 1999, **40**, 6609–6611.
11 T. Sato, *Bull. Chem. Research Inst. Non-Aqueous Solutions, Tohoku Univ.*, 1959, **8**, 47–62 (*Chem. Abs.*, 1960, 10509).
12 The average chemical shift for the cations **7a**,**b** was calculated by simply taking an average of the entire chemical shift values in the seven-membered ring without the distinction of the conformational isomers ***7A*** and ***7B***.
13 PM3 semi-emprical MO calculations were performed by MOPAC version 6 on a Tektronix CAChe WorkSystem.
14 (*a*) T. Asao and S. Ito, *J. Synth. Org. Chem., Jpn.*, 1996, **54**, 2–14; (*b*) S.-I. Takekuma, M. Tanizawa, M. Sasaki, T. Matsumoto and H. Takekuma, *Tetrahedron Lett.*, 2002, **43**, 2073–2078; (*c*) M. Sasaki, M. Nakamura, G. Hannita, H. Takekuma, T. Minematsu, M. Yoshihara and S.-I. Takekuma, *Tetrahedron Lett.*, 2003, **44**, 275–279; (*d*) M. Sasaki, M. Nakamura, T. Uriu, H. Takekuma, T. Minematsu, M. Yoshihara and S.-I. Takekuma, *Tetrahedron*, 2003, **59**, 505–516.
15 (*a*) R. C. Kerber and H. M. Hsu, *J. Am. Chem. Soc.*, 1973, **95**, 3239–3245; (*b*) K. Komatsu, K. Masumoto, Y. Waki and K. Okamoto, *Bull. Chem. Soc. Jpn.*, 1982, **55**, 2470–2479.